

AN EFFICIENT INVERSE SCATTERING ALGORITHM AND ITS APPLICATION TO LOSSY ELECTRIC TRANSMISSION LINE SYNTHESIS

H. Tang* and Q. Zhang

INRIA-IRISA, Campus de Beaulieu, Rennes Cedex 35042, France

Abstract—As studied by Jaulent in 1982, the inverse problem of lossy electric transmission lines is closely related to the inverse scattering of Zakharov-Shabat equations with two potential functions. Focusing on the numerical solution of this inverse scattering problem, we develop a fast one-shot algorithm based on the Gelfand-Levitan-Marchenko equations and on some differential equations derived from the Zakharov-Shabat equations. Compared to existing results, this new algorithm is computationally more efficient. It is then applied to the synthesis of non uniform lossy electric transmission lines.

1. INTRODUCTION

Electric transmission line synthesis consists in determining the physical parameters of a transmission line from a specified behavior for electric wave reflection and transmission [1–3]. This problem is studied for the design of microwave devices [4–6] and for the development of very large scale integrated (VLSI) circuits [7]. Based on the transformations from the telegrapher's equations of transmission lines to Zakharov-Shabat equations as studied in [8], the synthesis problem is related to the inverse scattering problem of the following coupled Zakharov-Shabat equations with two potential functions which will be referred to as ZS^+

$$ZS^+ : \begin{cases} \frac{d\nu_1(k, x)}{dx} + ik\nu_1(k, x) = q^+(x)\nu_2(k, x) & (1a) \\ \frac{d\nu_2(k, x)}{dx} - ik\nu_2(k, x) = q^-(x)\nu_1(k, x) & (1b) \end{cases}$$

where k is the wave number and $q^\pm(x)$ are two potential functions which are functions of distributed characteristic parameters of a

Received 7 January 2011, Accepted 31 March 2011, Scheduled 6 June 2011

* Corresponding author: Huaibin Tang (tanghuaibin@gmail.com).

transmission line. Solutions to the problem of transmission line synthesis based on the inverse scattering theory have been studied in [9, 10]. In the present paper a more efficient numerical solution is developed and more realistic numerical simulations are provided.

The inverse scattering problem consists in determining the potential functions $q^\pm(x)$ from reflection and transmission coefficients. Following the pioneering works reported in [11, 12], the solution to the inverse scattering problem can be computed, in principle, by solving linear integral equations, known as Gelfand-Levitan-Marchenko (GLM) equations.

Some numerical algorithms for solving inverse scattering problems have been proposed, for instance [13–16]. For the case that the two potential functions $q^\pm(x)$ are equal (in this case the ZS⁺ equations are referred to as Zakharov-Shabat equations with a single potential function), the related numerical algorithm is well developed. In [17], an efficient numerical algorithm was proposed by supplementing the GLM equations with some second order partial differential equations derived from Zakharov-Shabat equations to avoid full large size algebraic equations after the discretization of the GLM equations. However, this approach requires time consuming iterations to compensate the approximations made in the second order partial differential equations. This result is later improved by a more efficient one [18] where the second order partial differential equations supplementing the GLM equations are replaced by first order partial differential equations.

It is noted that when applied to electric transmission lines, the single-potential Zakharov-Shabat equations correspond to lossless lines [18, 19], whereas the two-potential equations cover the case of lossy lines [8, 9].

For the case that the two potential functions $q^\pm(x)$ are different, there exist several algorithms. In [9], the iterative numerical algorithm of [17] is extended to this more general case by supplementing the GLM equations with similar second order partial differential equations. The method proposed in [16] is based on the GLM equations only, with a special matrix inversion computation reusing the computations made in previous steps. In the present paper, inspired by the work of [18] for Zakharov-Shabat equations with a single potential function, we present an efficient one-shot numerical algorithm by simplifying the iterative algorithm of [9]. Compared to the algorithm of [9], the improvement of this new algorithm in terms of computational cost is similar to that of [18] compared to [17]. The algorithm of [16] has the advantage of being based on the GLM equations only, but our new algorithm is computationally less expensive.

The results presented in this paper are related to an earlier

work [20] (an enriched version can be found at <http://hal.archives-ouvertes.fr/inria-00511353/en/>) where the problem of fault diagnosis was studied, with the main focus on the issues between engineering practice and the inverse scattering theory. In that work, the potential functions of Zakharov-Shabat equations are used as a tool to reveal faults causing distributed variations of physical parameters, but the problem of retrieving physical parameters was not considered. The present paper is focused on the numerical inverse scattering algorithm. As an example of its application, the synthesis of lossy transmission lines will be studied by numerical simulation: distributed transmission line parameters will be computed from simulated scattering data, with the new numerical inverse scattering algorithm.

This paper is organized as follows. In Section 2, after a brief formulation of the inverse scattering problem for the generalized Zakharov-Shabat equations with two potential functions, the new numerical algorithm, extending the results of [9, 17, 18], will be presented. Its computational advantage is then investigated by comparing with existing algorithms. To illustrate the effectiveness of the presented new algorithm, it will be applied to the synthesis of non uniform lossy transmission lines in Section 3. Concluding remarks are made at Section 4.

2. A NEW NUMERICAL ALGORITHM FOR THE INVERSE SCATTERING PROBLEM

After a short recall of the inverse scattering problem related to the Zakharov-Shabat equations, an efficient one-shot numerical algorithm is presented in this section. Its computational cost is then compared with existing algorithms. The relationship between transmission line synthesis and the inverse scattering problem has been established in [8]. It will also be shortly recalled in Section 3.

2.1. Formulation of the Inverse Scattering Problem

To determine the coupling potential functions $q^\pm(x)$ from the scattering data of ZS^+ , we assume that ZS^+ has no bound state (square integrable solution for $x \in \mathbb{R}$), then the scattering data are composed of $r_l(k)$, $r_r(k)$, and $t(k)$, which are respectively the left reflection coefficient, the right reflection coefficient, and the transmission coefficient of ZS^+ .

Following [21], the solution of the inverse scattering problem for ZS^+ requires the left reflection coefficient $r_l(k)$ of ZS^+ , and also the left reflection coefficient $r_l^-(k)$ of the auxiliary system ZS^- which is

obtained by interchanging the two potential functions $q^\pm(x)$,

$$\text{ZS}^- : \begin{cases} \frac{d\nu_1^-(k, x)}{dx} + ik\nu_1^-(k, x) = q^-(x)\nu_2^-(k, x) & (2a) \\ \frac{d\nu_2^-(k, x)}{dx} - ik\nu_2^-(k, x) = q^+(x)\nu_1^-(k, x) & (2b) \end{cases}$$

We consider the case that ZS^\pm are casual systems, thus their impulse responses, i.e., the Fourier transforms of $r_l(k)$ and $r_l^-(k)$, namely $R_l(y)$ and $R_l^-(y)$, are equal to zeros for $y < 0$. This assumption implies that $q^\pm(x) = 0$ for all $x < 0$.

Following [21], the inverse scattering transform for the computation of $q^\pm(x)$ consists of the following steps:

- (1) Compute $r_l^-(k)$ from the scattering data of ZS^+ through

$$r_l^-(k) = \frac{r_r(-k)}{r_r(-k)r_l(-k) - (t(-k))^2} \quad (3)$$

- (2) Compute the Fourier transforms

$$R_l(y) = \frac{1}{2\pi} \int_{-\infty}^{+\infty} r_l(k)e^{-iky} dk, \quad R_l^-(y) = \frac{1}{2\pi} \int_{-\infty}^{+\infty} r_l^-(k)e^{-iky} dk$$

- (3) Solve the following GLM integral equations for the unknown kernel functions $A_{r_1}(x, y)$, $A_{r_2}(x, y)$, $A_{r_1}^-(x, y)$, and $A_{r_2}^-(x, y)$

$$A_{r_1}^-(x, y) + \int_{-y}^x ds A_{r_2}(x, s) R_l(y + s) = 0 \quad (4a)$$

$$A_{r_2}(x, y) + R_l^-(x + y) + \int_{-y}^x ds A_{r_1}^-(x, s) R_l^-(y + s) = 0 \quad (4b)$$

$$A_{r_1}(x, y) + \int_{-y}^x ds A_{r_2}^-(x, s) R_l^-(y + s) = 0 \quad (5a)$$

$$A_{r_2}^-(x, y) + R_l(y + x) + \int_{-y}^x ds A_{r_1}(x, s) R_l(y + s) = 0 \quad (5b)$$

- (4) Compute the potential functions $q^\pm(x)$ from

$$q^+(x) = 2A_{r_2}^-(x, x), \quad q^-(x) = 2A_{r_2}(x, x) \quad (6)$$

For more details about the inverse scattering theory, we refer the readers to [21].

2.2. Numerical Algorithm

For the above inverse scattering problem, as the computation of $r_l^-(k)$ from $r_l(k), r_r(k)$, and $t(k)$ is trivial, and the Fourier transforms $R_l(y)$ and $R_l^-(y)$ can be computed with the aid of fast Fourier transform (FFT) from sampled values of $r_l(k)$ and $r_l^-(k)$, the main numerical computations concern the solution of the GLM Equations (4), (5) for the kernel functions $A_{r_1}(x, y), A_{r_2}(x, y), A_{r_1}^-(x, y)$, and $A_{r_2}^-(x, y)$.

Inspired by the work reported in [18] for Zakharov-Shabat equations with a single potential function, we present an efficient one-shot numerical algorithm by simplifying the iterative algorithm of [9] for the inverse scattering problem formulated in the previous section. In this algorithm, the GLM Equations (4), (5) will be supplemented by the following two pairs of first order partial differential equation which are derived from ZS $^\pm$ ([21]):

$$\frac{\partial A_{r_1}(x, y)}{\partial x} + \frac{\partial A_{r_1}(x, y)}{\partial y} = q^+(x)A_{r_2}(x, y) \quad (7a)$$

$$\frac{\partial A_{r_2}(x, y)}{\partial x} - \frac{\partial A_{r_2}(x, y)}{\partial y} = q^-(x)A_{r_1}(x, y) \quad (7b)$$

$$\frac{\partial A_{r_1}^-(x, y)}{\partial x} + \frac{\partial A_{r_1}^-(x, y)}{\partial y} = q^-(x)A_{r_2}^-(x, y) \quad (8a)$$

$$\frac{\partial A_{r_2}^-(x, y)}{\partial x} - \frac{\partial A_{r_2}^-(x, y)}{\partial y} = q^+(x)A_{r_1}^-(x, y) \quad (8b)$$

As in [9, 17, 18], we introduce the coordinate change $\xi = (x + y)/2, \eta = (x - y)/2$ to transform the region of $x \geq |y|$ in the x - y plane to the first quadrant in the ξ - η plane. Also, the A -kernels will be rewritten as B -kernels after the coordinate change $A_{r_1}^-(x, y) = B_1^-(\xi, \eta), A_{r_2}^-(x, y) = B_2^-(\xi, \eta), A_{r_1}(x, y) = B_1(\xi, \eta), A_{r_2}(x, y) = B_2(\xi, \eta)$. Now discretize the grid on the ξ - η plane defined by $\xi = id$ and $\eta = jd$, with $i, j = 0, 1, 2, \dots$, and d being the discretization step size.[†] With $B_1(id, jd)$ be simply written as $B_1(i, j)$, and similarly for other values, the discrete counterparts of Equations (4)–(8) then write

$$B_1^-(i, j) = -2d \sum_{k=0}^{i-1} B_2(k + j, i - k)R_l(2k) \quad (9a)$$

$$B_2(i, j) = -R_l^-(2i) - 2d \sum_{k=0}^{i-1} B_1^-(k + j, i - k)R_l^-(2k) \quad (9b)$$

[†] The index notations i, j used here should not be confused with the imaginary unit number.

$$B_1(i, j) = -2d \sum_{k=0}^{i-1} B_2^-(k+j, i-k) R_l^-(2k) \quad (9c)$$

$$B_2^-(i, j) = -R_l(2i) - 2d \sum_{k=0}^{i-1} B_1(k+j, i-k) R_l(2k) \quad (9d)$$

$$q^+(i+j) = 2B_2^-(i+j, 0) \quad (9e)$$

$$q^-(i+j) = 2B_2(i+j, 0) \quad (9f)$$

$$B_1(i, j) = B_1(i-1, j) + dq^+(i+j-1)B_2(i-1, j) \quad (9g)$$

$$B_2(i, j) = B_2(i, j-1) + dq^-(i+j-1)B_1(i, j-1) \quad (9h)$$

$$B_1^-(i, j) = B_1^-(i-1, j) + dq^-(i+j-1)B_2^-(i-1, j) \quad (9i)$$

$$B_2^-(i, j) = B_2^-(i, j-1) + dq^+(i+j-1)B_1^-(i, j-1) \quad (9j)$$

with the boundary conditions

$$B_1^-(0, j) = 0, \quad B_2(0, \eta) = -R_l^-(0), \quad (10a)$$

$$B_2^-(0, j) = -R_l(0), \quad B_1(0, \eta) = 0 \quad (10b)$$

derived from the GLM Equations (4), (5) by setting $\xi = 0$.

In what follows, the L -th diagonal of the discretization grid will refer to the set of all the grid nodes (i, j) such that $i + j = L$ and $i, j \geq 0$. For any node (i, j) on diagonal L of the grid, we say the kernel value $B_1(i, j)$ is on diagonal L , so are the other similar kernel values and the potential function values. With Equations (9g)–(9j) which relate the kernel values in successive diagonals, Equations (9b)

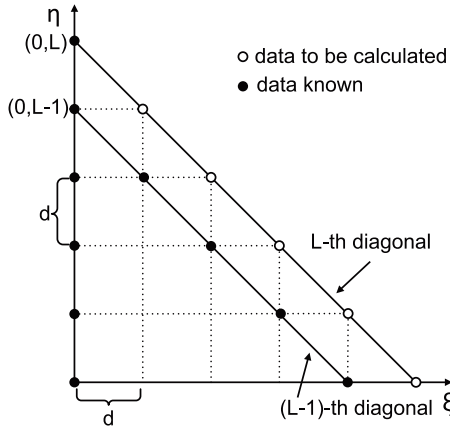


Figure 1. Grid structure for the inverse scattering algorithm.

and (9d) which relate all the kernel values on a same diagonal, and the boundary conditions (10), the kernel and potential function values can be computed diagonal by diagonal, by repeatedly increasing the value of L . To illustrate the discretization of the coordinate system ξ - η and the calculation of the kernel values, Fig. 1 is adopted from [18].

The complete algorithm is summarized as follows.

- At diagonal $L = 0$, apply the boundary conditions (10),

$$B_1^-(0, 0) = 0, \quad B_2^-(0, 0) = -R_l(0), \quad B_1(0, 0) = 0, \quad B_2(0, 0) = -R_l^-(0)$$
 and compute the first potential values from (9e) and (9f),

$$q^+(0) = 2B_2^-(0, 0) = -2R_l(0), \quad q^-(0) = 2B_2(0, 0) = -2R_l^-(0)$$
- For $L = 1, 2, 3, \dots$, the nodes (i, j) on diagonal L are such that $i + j = L$.
 - (1) Initialize with the boundary conditions (10) by $B_1^-(0, L) = 0$, $B_2^-(0, L) = -R_l(0)$, $B_1(0, L) = 0$, $B_2(0, L) = -R_l^-(0)$.
 - (2) Use (9g) and (9i) to find all the other values of $B_1(i, j)$ and $B_1^-(i, j)$, and use (9h) and (9j) to find all the other values of $B_2(i, j)$ and $B_2^-(i, j)$, except $B_2(L, 0)$ and $B_2^-(L, 0)$.
 - (3) Compute $B_2(L, 0)$ and $B_2^-(L, 0)$ through (9b) and (9d).
 - (4) Compute $q^+(L)$ and $q^-(L)$ through (9e) and (9f):

$$q^+(L) = 2B_2^-(L, 0), \quad q^-(L) = 2B_2(L, 0).$$
- Stop if L reaches the maximum size of the discretization grid; otherwise increase L by one, then go back to the last step.

2.3. Computational Cost of the New Algorithm

In the above new algorithm, to accomplish the computation on the L -th diagonal, the Equations (9g) and (9i) will be used L times each, (9h) and (9j) $(L - 1)$ times each, (9d), (9b), (9e) and (9f) one time each. Thus the computational cost on the diagonal L is $O(L)$. When the computation is made on a discretization grid of size N , the number of diagonals is N . The computation cost on each diagonal is $O(L)$ for $L = 1, 2, \dots, N$. It follows that the whole algorithm has a computational cost not more than $O(N^2)$. For the iterative algorithm in [9], the computational cost of its initialization step is also at the order of $O(N^2)$, but this step is followed by an iterative algorithm to compensate the approximations made in the initialization step. Each of these iterations costs $O(N^3)$. The computational cost of the algorithm of [16] is not less than $O(N^3)$, despite its wise matrix inversion method. Compared to these results, our new algorithm is computationally more

efficient. In these comparisons, it is also worth mentioning that the algorithm of [16] is based on the GLM equations only.

To illustrate the effectiveness of our algorithm, we will apply it to the synthesis of lossy electric transmission lines in the next section.

3. THE SYNTHESIS OF LOSSY ELECTRIC TRANSMISSION LINES

Consider the case that the transmission line is composed of a pair of conductors separated by a high quality insulation material. In this case the leakage between the two conductors is neglected, and a transmission line is characterized by its distributed inductance $L(z)$, capacitance $C(z)$, and series resistance $R(z)$ along the longitudinal coordinate z . It is not possible to determine individually these three characteristic parameters from specified reflection and transmission coefficients, hence only the ratios $L(z)/C(z)$ and $R(z)/L(z)$ will be computed.

For a considered lossy transmission line, the voltage $U(k, z)$ and the current $I(k, z)$ at any point z are governed by the frequency domain telegrapher's equations:

$$\frac{dU(k, z)}{dz} - ikL(z)I(k, z) + R(z)I(k, z) = 0 \quad (11a)$$

$$\frac{dI(k, z)}{dz} - ikC(z)U(k, z) = 0 \quad (11b)$$

Under the Liouville transformation $x(z) = \int_0^z \sqrt{L(s)C(s)} ds$ replacing the space coordinate z , and after the changes of variables as defined in [8], the telegrapher's Equations (11) are transformed to the Zakharov-Shabat equations as already formulated in (1), with the *two* potential functions

$$q^\pm(x) = \left(-\frac{1}{4} \frac{d}{dx} \left(\ln \frac{L(x)}{C(x)} \right) \mp \frac{1}{2} \frac{R(x)}{L(x)} \right) \exp \left(\mp \int_{-\infty}^x \frac{R(y)}{L(y)} dy \right) \quad (12)$$

With the numerical method presented in Subsection 2.2, the two potential functions $q^\pm(x)$ expressed in (12) can be computed from specified scattering data[‡] $r_l(k)$, $r_r(k)$, and $t(k)$. The next step is then to inverse the equalities (12) for the ratios $L(x)/C(x)$ and $R(x)/L(x)$.

To determine the ratios $L(x)/C(x)$ and $R(x)/L(x)$ which represent the characteristic properties of the transmission line, define

[‡] In practice the specified reflection and transmission coefficients have their engineering definitions. Their equivalence to the theoretic definitions used in the inverse scattering theory are discussed in the our previous work (<http://hal.archives-ouvertes.fr/inria-00511353/en/>).

the auxiliary function $g(x) = \exp(-\int_{-\infty}^x R(y)/L(y)dy)$ and notice that, following (12), it satisfies the Riccati equation

$$\frac{dg(x)}{dx} = q^+(x) - q^-(x)g(x)^2 \tag{13}$$

After numerically solving for $g(x)$ from (13), the ratios $L(x)/C(x)$ and $R(x)/L(x)$ can be calculated as

$$\frac{L(x)}{C(x)} = \frac{L(-\infty)}{C(-\infty)} \left(\exp \left(-4 \int_{-\infty}^x q^-(y)g(y)dy \right) + \frac{1}{g(x)^2} \right) \tag{14}$$

$$\frac{R(x)}{L(x)} = -\frac{d \ln g(x)}{dx} \tag{15}$$

In the following numerical examples, the reflection and transmission coefficients will be generated by a numerical simulator of transmission lines, so that the result of transmission line synthesis from the simulated scattering data can be compared to the transmission line characteristic parameters used in the simulator.

Example 1. We consider a lossy transmission line of length 1 km with $L = 0.9 \mu\text{H}/\text{m}$ and $C = 0.1 \text{nF}/\text{m}$ (constant values). The variation of $R(x)$ in the form of R/L is depicted in Fig. 2. Firstly, we simulate the scattering data of the transmission line by the numeric simulator as described in Section 3.1 in our previous work (<http://hal.archives-ouvertes.fr/inria-00511353/en/>), and they are shown in Fig. 3 and Fig. 4. Then, the scattering data $r_l(k)$ and $r_l^-(k)$ required by the inverse scattering problem can be calculated through Proposition 2 in our previous work (<http://hal.archives-ouvertes.fr/inria-00511353/en/>). With the numeric algorithm described in Subsection 2.2, the two potential functions $q^\pm(x)$ are computed. At last, the ratios $L(x)/C(x)$ and $R(x)/L(x)$ can be obtained through (13)–(15). As shown in Fig. 2, the results obtained by solving the inverse scattering problem accord well with the true values.

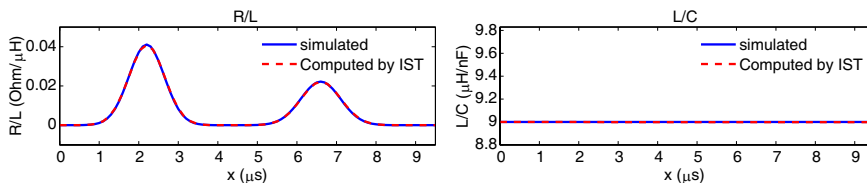


Figure 2. R/L and L/C computed by the inverse scattering algorithm, and compared with the true values (Example 1).

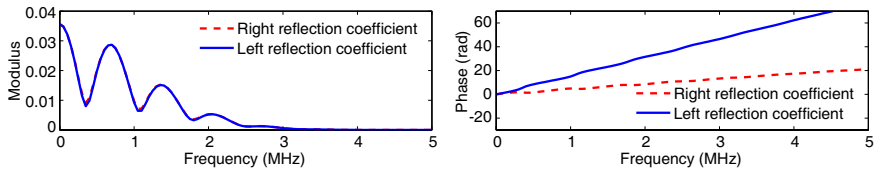


Figure 3. Simulated reflection coefficients (Example 1).

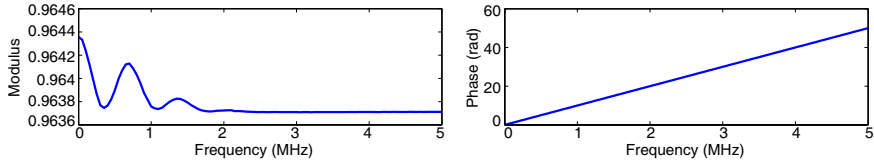


Figure 4. Simulated transmission coefficient (Example 1).

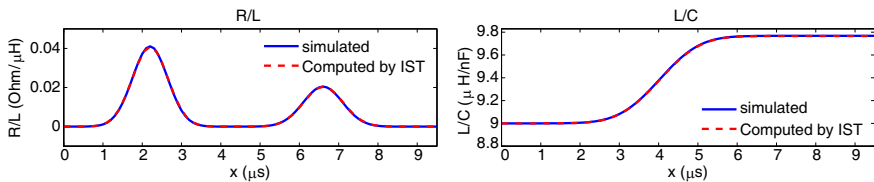


Figure 5. R/L and L/C computed by the inverse scattering algorithm, and compared with the true values (Example 2).

Example 2. As a second example, we consider the case that the profile of $L(x)/C(x)$ is smoothly increasing and the other parameters of the transmission line remain the same as in the above example. The simulated scattering data of the transmission line are plotted in Fig. 6, Fig. 7, and Fig. 8 (in solid line) and the characteristic parameter profiles computed through the inverse scattering problem are compared to the original profiles in Fig. 5. Again, the ratios $L(x)/C(x)$ and $R(x)/L(x)$ are correctly retrieved by the inverse scattering algorithm.

Example 3. To evaluate the stability of our inverse scattering algorithm when the scattering data are randomly disturbed, we repeat the second simulation example by adding white Gaussian noises to each simulated scattering data. The signal-to-noise-ratio (SNR) is 10 dB for the simulated scattering data. The noise-corrupted scattering data are illustrated in Fig. 6, Fig. 7, and Fig. 8 (in dashed line). From the significantly noise-corrupted scattering data, the ratios $L(x)/C(x)$ and $R(x)/G(x)$ are computed again from the inverse scattering algorithm. As illustrated in Fig. 9, the profiles are reasonably retrieved.

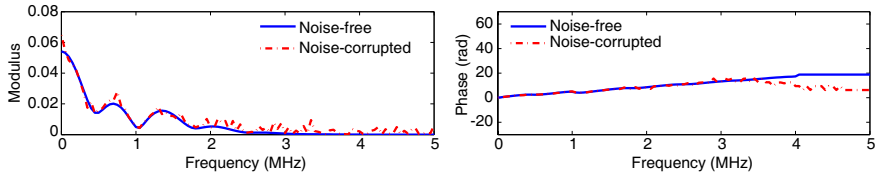


Figure 6. Simulated left reflection coefficients, the noise-free case in solid line (Example 2), and the noise-corrupted case in dashed line (Example 3).

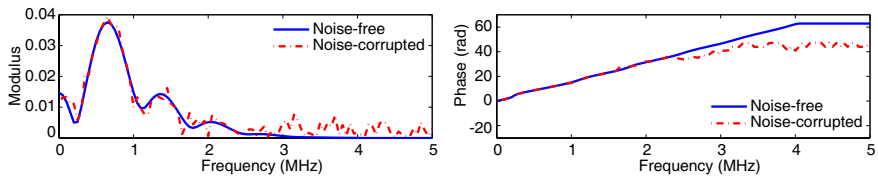


Figure 7. Simulated right reflection coefficients, the noise-free case in solid line (Example 2), and the noise-corrupted case in dashed line (Example 3).

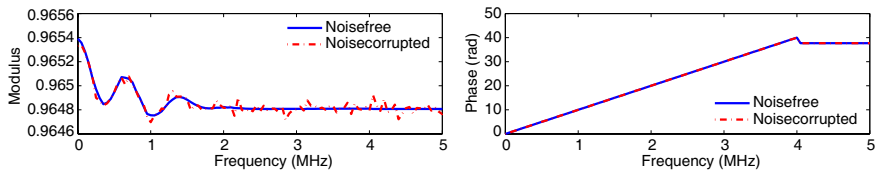


Figure 8. Simulated transmission coefficient, the noise-free case in solid line (Example 2), and the noise-corrupted case in dashed line (Example 3).

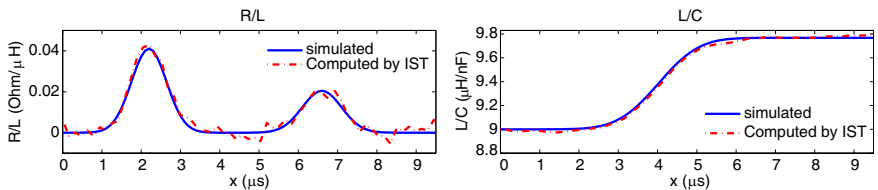


Figure 9. R/L and L/C computed by the inverse scattering algorithm from the noise-corrupted scattering data (Example 3).

Though in theory the scattering data are required for frequency ranging from 0 to $+\infty$, in practice it has to be truncated to a finite bandwidth. In the above simulation results, the values of the reflection coefficients are close to 0 after 5 MHz, thus the bandwidth from 0 to 5 MHz has been sufficient. For practical experiments, this is a relatively narrow bandwidth, since conventional network analyzers can cover up to 1000 MHz (1 GHz).

4. CONCLUSION

In this paper, through the approach of solving the inverse scattering problem related to the Zakharov-Shabat equations with two potential functions, an efficient numerical algorithm for the synthesis of lossy transmission lines is presented. Inspired by the work of [18] on Zakharov-Shabat equations with a single potential function, the second order partial differential equations derived from Zakharov-Shabat equations used in the algorithm of [9] are replaced by first order partial differential equations. This modification has the advantage of leading to a large triangular set of linear algebraic equations, hence these equations can be efficiently solved by a one-shot algorithm, instead of the iterative algorithm used in [9].

Compared to existing results, our numerical algorithm has a great advantage in terms of numerical computation, since its cost is at the order of $O(N^2)$, whereas the other existing algorithms are at least of $O(N^3)$. Its effectiveness is also illustrated by the numerical simulations for transmission line synthesis.

ACKNOWLEDGMENT

This work has been supported by the ANR INSCAN project.

REFERENCES

1. Lin, C. J., C. C. Chiu, S. G. Hsu, and H. C. Liu, "A novel model extraction algorithm for reconstruction of coupled transmission lines in high-speed digital system," *Journal of Electromagnetic Waves and Applications*, Vol. 19, No. 12, 1595–1609, 2005.
2. Lundstedt, J. and M. NorgrenLin, "Comparison between frequency domain and time domain methods for parameter reconstruction on nonuniform dispersive transmission lines," *Progress In Electromagnetics Research*, Vol. 43, 1–37, 2003.

3. Sheen, D. and D. Shepelsky, "Uniqueness in the simultaneous reconstruction of multiparameters of a transmission line," *Progress In Electromagnetics Research*, Vol. 21, 153–172, 1999.
4. Bilotti, F., L. Vegni, and A. Toscano, "A new stripline high pass filter layout," *Journal of Electromagnetic Waves and Applications*, Vol. 14, No. 3, 423–439, 2000.
5. Costanzo, S., "Synthesis of multi-step coplanar waveguide-to-microstrip transition," *Progress In Electromagnetics Research*, Vol. 113, 111–126, 2011.
6. Monti, G., R. De Paolis, and L. Tarricone, "Design of a 3-state reconfigurable CRLH transmission line based on mems switches," *Progress In Electromagnetics Research*, Vol. 95, 283–297, 2009.
7. Mao, J. F., O. Wing, and F. Y. Chang, "Synthesis of coupled transmission lines," *IEEE Transactions on Circuits and Systems I: Fundamental Theory and Applications*, Vol. 44, No. 4, 327–337, 1997.
8. Jaulent, M., "The inverse scattering problem for LCRG transmission lines," *Journal of Mathematical Physics*, Vol. 23, No. 12, 2286–2290, 1982.
9. Frangos, P. V. and D. L. Jaggard, "Analytical and numerical solution to the two-potential Zakharov-Shabat inverse scattering problem," *IEEE Transactions on Antennas and Propagation*, Vol. 40, No. 4, 399–404, 1992.
10. Xiao, G. B. and K. Yashiro, "An improved algorithm of constructing potentials from cauchy data and its application in synthesis of nonuniform transmission lines," *IEEE Transactions on Microwave Theory and Techniques*, Vol. 50, No. 8, 2025–2028, 2002.
11. Gelfand, I. M. and B. M. Levitan, "On the determination of a differential equation by its spectral function," *American Mathematical Society Translations*, Vol. 1, 253–304, 1955.
12. Marchenko, V. A., "Reconstruction of the potential energy from the phase of scattered waves," *Dokl. Akad. Nauk. SSR*, Vol. 104, 635–698, 1955.
13. Frangos, P. V., "One-dimensional inverse scattering: Exact methods and applications," Ph.D. Thesis, University of Pennsylvania, 1986.
14. Frangos, P. V. and D. L. Jaggard, "Inverse scattering: Solution of coupled Geland-Levitan-Marchenko integral equations using successive kernel approximations," *IEEE Transactions on Antennas and Propagation*, Vol. 43, No. 6, 547–552, 1995.

15. Song, G. H. and S. Y. Shin, "Design of corrugated waveguide filters by the Gelfand-Levitan-Marchenko inverse-scattering method," *Journal of the Optical Society of America. A, Optics, Image Science, and Vision*, Vol. 2, 1905–1915, 1985.
16. Modelski, J. and A. Synyavskyy, "A new numerical method for Zakharov-Shabat's inverse scattering problem solution," *International Conference on Microwaves, Radar and Wireless Communications*, Krakow, 2006.
17. Frangos, P. V., and D. L. Jaggard, "A numerical solution to the Zakharov-Shabat inverse scattering problem," *IEEE Transactions on Antennas and Propagation*, Vol. 39, No. 1, 74–79, 1991.
18. Xiao, G. B. and K. Yashiro, "An efficient algorithm for solving Zakharov-Shabat inverse scattering problem," *IEEE Transactions on Antennas and Propagation*, Vol. 50, No. 6, 807–811, 2002.
19. Zhang, Q. H., M. Sorine, and M. Admane, "Inverse scattering for soft fault diagnosis in electric transmission lines," *IEEE Transactions on Antennas and Propagation*, Vol. 59, No. 1, 141–148, 2011.
20. Tang, H. B. and Q. H. Zhang, "Inverse scattering for lossy electric transmission line soft fault diagnosis," *IEEE Antennas and Propagation Society International Symposium*, Toronto, 2010.
21. Eckhaus, W. and A. V. Harten, *The Inverse Scattering Transformation and the Theory of Solitons: An Introduction*, Elsevier, 1981.